

Ammonia and nitrite oxidation in the upper euphotic zone of the oligotrophic Red Sea

Eyal Rahav^{1,2,3*}, Scott D Wankel⁴, and Adina Paytan²

¹ Israel Oceanographic and Limnological Research, Haifa, Israel.

² Institute of Marine Science, University of California, Santa Cruz, CA, USA.

³ Department of Earth and Environmental Science, Ben-Gurion University of the Negev, Beer Sheva, Israel.

⁴ Marine Chemistry and Geochemistry Department, Woods Hole Oceanographic Institution, Woods Hole, Massachusetts, USA.

*Corresponding author: eyrahav@ucsc.edu; eyal.rahav@ocean.org.il

Abstract

Nitrification is widely understood to be inhibited by light in the surface ocean, however, increasing evidence indicates its occurrence at low levels at many sites. The extent to which nitrification remains active in the euphotic zone could have important implications to new production calculations, yet it remains understudied. Here, we quantified ammonia and nitrite oxidation rates in the euphotic zone of the Gulf of Aqaba (Northern Red Sea) from late spring to late summer and examined environmental controls and implications for dark carbon fixation (chemoautotrophy) and new production. Both ammonia and nitrite oxidation were detectable throughout the euphotic zone ($\sim 0.1\text{-}0.8\text{ nmol N L}^{-1}\text{ d}^{-1}$). Overall, rates were low in the highest-irradiance surface waters and increased with depth. Integrated rates over the entire euphotic zone ($24\text{-}56\text{ }\mu\text{mol N m}^{-2}\text{ d}^{-1}$) were among the lowest reported for oligotrophic regions globally. This reflects extremely low substrate concentrations and intense, though not complete, photo-inhibition. Ammonia and nitrite oxidation together supported $<2\%$ of dark carbon fixation rates, suggesting other processes, not accounted for, drive this chemoautotrophic activity. Depth-resolved correlations with environmental parameters highlight light, temperature, and substrate availability as key regulators of both processes. Our results show that nitrification in the Gulf of Aqaba operates at the lower bounds of global euphotic zone rates and is loosely coupled to carbon cycling. These findings underscore the need to better resolve nitrification dynamics in ultra-oligotrophic, rapidly warming, seas to refine estimates of new production and chemoautotrophic carbon assimilation under future ocean conditions.

33

34 **Key words:** Ammonia oxidation, Nitrite oxidation, Dark carbon fixation, Red Sea,
35 Oligotrophic marginal seas.

36

37 **1 Introduction**

38 Nitrification, the sequential oxidation of ammonium (NH_4^+) to nitrite (NO_2^-) followed
39 by the oxidation of nitrite to nitrate (NO_3^-), is a microbially mediated process central to the
40 regulation of nitrogen availability across nearly all aquatic environments, linking the most
41 reduced and oxidized states of nitrogen (Ward, 2008). Although nitrification does not change
42 the absolute inventory of bioavailable nitrogen (N) in the oceans, it alters the balance among
43 nitrogen species that serve as substrates for different organisms, thereby affecting
44 phytoplankton species abundance and growth (Fawcett et al., 2011). Ammonia oxidation is
45 carried out by ammonia-oxidizing archaea and bacteria (Francis et al., 2005; Wuchter et al.,
46 2006), while nitrite oxidation is performed by nitrite-oxidizing bacteria (Mincer et al., 2007;
47 Pachiadaki et al., 2017). Ammonia-oxidizing bacteria that perform the entire process have also
48 been identified in freshwater, terrestrial, and coastal habitats, but have not yet been found in
49 the open ocean (Daims et al., 2015; Fei et al., 2018; van Kessel et al., 2015).

50 Nitrification has been investigated across a wide range of marine settings, including the
51 Atlantic (Clark et al., 2008, 2022), the Pacific (Wan et al., 2021; Wankel et al., 2007), and the
52 Polar (Mdutyana et al., 2020; Shiozaki et al., 2019) ocean basins, as well as numerous coastal
53 and estuarine systems (Henriksen and Kemp, 1988; Herbert, 1999; Zhu et al., 2018). As a
54 chemoautotrophic process, nitrification contributes to organic carbon production in the ocean
55 interior (Middelburg, 2011; Pachiadaki et al., 2017), and may fuel bacterial carbon demand and
56 support heterotrophic food-webs in the mesopelagic and bathypelagic water depths (Bayer et
57 al., 2025). The activity of nitrifiers is known to be promoted or inhibited by many
58 environmental factors (Ward, 2008), yet specific controls on its occurrence in the water column
59 and broader ecological implications across different ocean settings remain poorly constrained
60 (Tang et al., 2023). Additionally, because uptake of NH_4^+ and NO_3^- has long served to
61 differentiate between ‘regenerated’ and ‘new’ production, respectively (Eppley and Peterson,
62 1979), *in situ* production of NO_3^- by nitrification in the photic zone skews global estimates of
63 new production and carbon export in the oceans (Yool et al., 2007; Wankel et al., 2007).

64 Here, we report ammonia and nitrite oxidation rates in the upper euphotic zone (surface
65 and down to ~100 m, representing 100% to ~0.5-1.8% of surface irradiance, respectively) of

66 the Gulf of Aqaba (GoA, Northern Red Sea) during late spring and throughout the summer
67 season. Rates were compared with common environmental physiochemical and biological
68 parameters to assess drivers of nitrification in this marine setting. Using these data, we provide
69 estimates of the contribution of ammonia and nitrite oxidation to dark carbon fixation (DCF)
70 and new production in the oligotrophic, warm and well-lit GoA.

71 **2 Material and methods**

72 Seawater was collected every 20 m throughout the euphotic zone (0-100 m depth) at an
73 offshore, routinely monitored, station in the GoA ("Station A", latitude 29.47 N, longitude
74 34.92 E). Ammonia and nitrite oxidation rates were assessed using stable ^{15}N isotope
75 enrichment incubations. Five monthly sampling events were performed spanning late
76 spring/early summer (May) to late summer (September) in 2023, covering the period in which
77 the GoA is characterized by oligotrophic N-poor conditions (Fuller et al., 2005; Mackey et al.,
78 2007). Ancillary water column measurements included temperature, salinity, photosynthetic
79 active radiation (PAR) (Seabird 19 Plus), inorganic nitrogen species concentrations (NO_2^- ,
80 NO_3^- , NH_4^+), chlorophyll-*a*, and rates of photosynthesis and DCF.

81 **2.1 Inorganic nitrogen species**

82 Duplicate water samples for nitrite (NO_2^-) and nitrate (NO_3^-) were collected in 15 ml
83 acid-clean polyethylene tubes directly from Niskin bottles. Prior to filling, the tube was
84 thoroughly rinsed three times with sample water. After collection, samples were stored at 4 °C
85 in the dark and analyzed the following day. Nitrite and nitrate concentrations were determined
86 colorimetrically following standard procedures (Grasshoff et al., 1999). Nitrite was measured
87 directly using the Griess reaction, in which nitrite forms an azo dye after reaction with
88 sulfanilamide and N-(1-naphthyl)ethylenediamine and is quantified spectrophotometrically
89 ($\lambda=520$ nm). Nitrate was reduced to nitrite using a copper-coated cadmium reduction column
90 and subsequently $\text{NO}_2^- + \text{NO}_3^-$ was analyzed by the same azo-dye method. Nitrate
91 concentrations were then calculated by difference. Analyses were performed using a Flow
92 Injection Autoanalyzer system (FIA, Lachat Instruments Model QuikChem 8000). The analysis
93 was automated, and peak areas were calibrated using standards prepared in nutrient-deplete
94 0.2- μm filtered surface seawater from the GoA over a range of 0-100 nmol L^{-1} . The detection
95 limits were 10 nmol L^{-1} and 20 nmol L^{-1} for nitrite and nitrate, respectively, with typical
96 analytical precision of ~ 20 nmol L^{-1} , consistent with previous measurements in the GoA (e.g.,
97 Mackey et al., 2011).

98 Samples for ammonia (NH_4^+) concentration were collected directly from Niskin bottles
99 into acid-washed plastic vials after rinsing 3 times with sample water. The collected samples
100 were stored in 4 °C in the dark and analyzed within an hour after collection. Ammonia
101 concentrations were determined using the orthophthaldialdehyde (OPA) method (Holmes et al.,
102 1999), where samples were first incubated with a working reagent of OPA for 3 h and then
103 measured fluorometrically (Turner Designs, Ex: 360 nm, Em. 420 nm). The detection limit was
104 $\sim 4 \text{ nmol L}^{-1}$ (Meeder et al., 2012). Procedural blanks were routinely measured and subtracted
105 from sample signals to account for background contamination. Note that calibration and quality
106 control procedures were carried out during nutrient measurements. The analytical precision and
107 detection limits were within the expected range for oligotrophic seawater measurements.

108 **2.2 Ammonia and nitrite oxidation rates**

109 Ammonia and nitrite oxidation rates were determined using stable isotope tracer
110 incubations (Beman et al., 2011; Bristow et al., 2015; Ward, 1987). Seawater was collected into
111 triplicate 1-L acid-cleaned transparent Nalgene bottles without headspace. The bottles were
112 incubated on land for 24 h in aquarium tanks continuously supplied with running surface
113 seawater, using neutral density screening nets simulating the light conditions of the collection
114 depth (no change in spectra). For ammonia oxidation, samples were amended with ^{15}N -labeled
115 ammonium chloride ($^{15}\text{NH}_4\text{Cl}$, >98 atom %; Cambridge Isotope Laboratories) at a
116 concentration of $\sim 20 \text{ nmol L}^{-1}$ which is sufficient to yield a quantifiable signal while potentially
117 introducing some degree of tracer perturbation (discussed below). For nitrite oxidation,
118 samples were amended with $\sim 5 \text{ nmol L}^{-1}$ of ^{15}N -labeled sodium nitrite ($^{15}\text{NO}_2^-$, >98 atom %),
119 thus minimally perturbing the *in situ* nitrite pool. At the end of the incubation, subsamples were
120 filtered onto a Supor 0.22 μm (47 mm) filter using gentle filtration, and the filtrate ($< 0.22 \mu\text{m}$)
121 was kept frozen in the dark at $-20 \text{ }^\circ\text{C}$ until analysis. For ammonia oxidation, the presence of
122 $^{15}\text{NO}_2^-$ in the total dissolved nitrite pool was quantified by isotope ratio mass spectrometry
123 (IRMS).

124 For nitrite oxidation, we quantified the $^{15}\text{NO}_3^-$ in the dissolved nitrate pool after
125 conversion to nitrous oxide with subsequent IRMS analysis. The azide method (McIlvin and
126 Altabet, 2005) and the denitrifier method (Casciotti et al., 2002; Sigman et al., 2001), with
127 technical updates for low-concentration analysis (McIlvin and Casciotti, 2011), are well
128 established for isotopic analysis of nitrite and nitrate in oligotrophic seawater. Prior to
129 denitrifier analysis, nitrite was removed from nitrate samples using the sulfamic acid procedure
130 (Granger and Sigman, 2009) to ensure that the ^{15}N signal reflected only the nitrate

131 pool. Aliquots of 2-10 ml were introduced per denitrifier vial depending on ambient NO_3^-
 132 concentration, consistent with the volume constraints of Sigman et al., (2001) and McIlvin and
 133 Casciotti, (2011). For surface samples with the lowest NO_3^- concentrations sequential injections
 134 of multiple aliquots from the same filtrate were used to accumulate sufficient N mass per vial,
 135 while for deeper samples with higher NO_3^- single injections of 2-5 ml were sufficient. Given
 136 that ambient NO_3^- and NO_2^- concentrations in GoA surface waters approached, or were below,
 137 the validated concentration ranges of these methods, the analyses were performed with careful
 138 attention to blank correction. Accordingly, rates derived from near-surface, low-concentration
 139 samples were interpreted conservatively. For sequential-injection analyses of low-
 140 concentration surface samples, multiple small-volume aliquots from the same 1-L filtrate were
 141 introduced into the same denitrifier vial to accumulate sufficient N mass, and the cumulative
 142 bacterial blank was estimated based on injection number and subtracted accordingly; samples
 143 where the ^{15}N signal could not be distinguished from the cumulative blank were excluded and
 144 treated as below the detection limit. In the most oligotrophic surface samples these established
 145 approaches were applied near their practical detection limits, and ^{15}N enrichments should
 146 therefore be regarded as conservative minimum estimates rather than evidence that the bacterial
 147 and azide methods are routinely robust at concentrations of only a few tens of nmol L^{-1} .

148 Killed controls poisoned with HgCl_2 from each collection depth were incubated in
 149 parallel to the experimental bottles to account for any abiotic transformations and subtracted
 150 from the ‘live’ bottles. Rates in the ‘mercury-killed’ controls were typically negligible relative
 151 to the ‘live’ bottles (usually $<0.05 \text{ nmol N L}^{-1} \text{ d}^{-1}$). The resulting detection limit, which was
 152 defined as the mean killed-control rate plus three standard deviations, corresponded to 0.1 nmol
 153 $\text{N L}^{-1} \text{ d}^{-1}$. Rates below this threshold were considered indistinguishable from background signal
 154 and were interpreted as ‘below detection’. This operational detection limit is based on the
 155 variability of killed controls and background signals and does not represent a full validation of
 156 isotope analysis at ambient nitrite or nitrate concentrations of only a few tens of nmol L^{-1} .
 157 Rates of ammonia and nitrite oxidation were calculated following previous studies (Beman et
 158 al., 2011; Bristow et al., 2015; Ward, 1987) as shown in Equations 1-3:

159
 160 (1) Ammonia oxidation = $\frac{\Delta (\text{atm}\% \text{ } ^{15}\text{N NO}_2) \times [\text{NO}_2]_{\text{final}}}{t \times F (\text{NH}_4)}$

161
 162 (2) Nitrite oxidation = $\frac{\Delta (\text{atm}\% \text{ } ^{15}\text{N NO}_3) \times [\text{NO}_3]_{\text{final}}}{t \times F (\text{NO}_2)}$

163

164 (3) $F_{\text{substrate}} = \frac{[^{15}\text{N substrate}]_{\text{added}}}{[\text{Substrate ambient}] + [\text{Substrate added}]}$

165

166 Where, $\Delta(\text{atm}\% \text{ } ^{15}\text{N NO}_2^-)$ or $\Delta(\text{atm}\% \text{ } ^{15}\text{N NO}_3^-)$ = atom% excess ^{15}N in the nitrite or nitrate
167 pool relative to natural abundance; $[\text{NO}_2^-]_{\text{final}}$ or $[\text{NO}_3^-]_{\text{final}}$ = final concentration of the nitrite
168 or nitrate pool (nmol L^{-1}); t = time (d); F_{NH_4} or F_{NO_2} = fractional ^{15}N enrichment of the ammonia
169 or nitrite substrate pool.

170

171 Note that for the ammonia oxidation rates we added tracer additions which correspond
172 to 30-50% of the ambient NH_4^+ concentrations. While we aimed to minimize substrate
173 perturbation, such additions are inherently challenging in ultra-oligotrophic systems, where
174 even low absolute tracer concentrations can represent a substantial fraction of the ambient pool
175 (Zheng et al., 2020). Consequently, the reported rates should be considered as potential rates
176 under moderately enriched conditions rather than strictly *in situ* rates (Dodds and Jones, 1987).
177 Additionally, incubations were conducted over 24 h, which may allow for processes such as
178 ammonia regeneration, microbial turnover, and grazing to influence substrate availability and
179 isotopic dilution. Although HgCl_2 -poisoned controls and parallel measurements were used to
180 account for abiotic and background signals, these incubations cannot fully resolve short-term
181 dynamics or transient coupling between regeneration and oxidation processes. These
182 methodological constraints are inherent to low-rate measurements in oligotrophic systems
183 (Ward, 1985) and should be considered when interpreting the results. Another potential caveat
184 arising from the 24 h incubation is the potential production of unlabelled nitrite via
185 phytoplankton nitrate reduction (e.g., Travis et al., 2024) thereby diluting the $^{15}\text{NO}_2^-$ pool
186 leading to an underestimation of both ammonia and nitrite oxidation rates. In the present study,
187 however, primary production and ambient nitrite concentrations were low, suggesting that this
188 effect was likely limited in magnitude.

189

190 **2.3 Photosynthesis and Dark Carbon Fixation (DCF)**

191 Photosynthesis and chemoautotrophic DCF rates were measured using $\text{NaH}^{14}\text{CO}_3$
192 incorporation method (Steemann-Nielsen, 1952) with minor modifications (Reich et al., 2024,
193 2026). Triplicate seawater samples were collected from Niskin bottles in 50 ml acid-washed
194 falcon tubes and spiked with a diluted ‘working solution’ of $\text{NaH}^{14}\text{CO}_3$ (Perkin Elmer, specific
195 activity 56 mCi mmol^{-1}) at a final radioisotope dilution of 1:10⁴ v:v. Tubes were incubated in
196 the same tanks and under the same conditions used for the ammonia and nitrite oxidation

197 measurements with one exception – the DCF bottles were first covered with aluminum foil to
198 prevent light penetration. The tubes were incubated for 24 h before being filtered onto GF/F
199 filters (0.7 μm nominal pore size, 25 mm diameter) using low vacuum pressure (<50 mmHg).
200 The filters were placed in glass scintillation vials and 50 μl of 37% hydrochloric acid was added
201 to remove the non-fixed ^{14}C -bicarbonate overnight. Scintillation cocktail (5 ml, ULTIMA-
202 GOLD) was then added to each vial and samples were counted using a TRI-CARB 4810 TR
203 (Packard) liquid scintillation counter. Additional T_0 blanks were prepared by spiking bottles
204 with $\text{NaH}^{14}\text{CO}_3$ and filtering immediately (without incubation). Blanks consistently yielded
205 negligible activity. Added activity was measured by withdrawing 50 μl from random spiked
206 bottles (immediately after dosing and before incubation) and adding it onto a new GF/F filter
207 with 50 μl of ethanolamine ($\text{pH}\approx 12$) followed by scintillation cocktail and counting
208 immediately.

209 Photosynthesis was calculated as the difference between the disintegration per minute
210 (DPM) measured in the samples incubated under ambient irradiance and the dark bottles. DCF
211 and photosynthesis rates were calculated based on the Bermuda Atlantic Time-series Study
212 (BATS) protocol using the following Equation 4:

213 (4) $Production = \frac{(DPM-blank)}{V} \times DIC \times \frac{AA\ vol}{TDPM} \times f \times \frac{1}{t}$

214 Where, DPM equals the disintegrations per minute, V = the filtered volume (50 ml), DIC is the
215 dissolved inorganic carbon in seawater ($\sim 25\ \text{mg C L}^{-1}$, similar to other oceanic sites, (Knap and
216 Michaels, 1993), AA vol = Added activity volume (50 μl), TDPM = Total ^{14}C disintegration
217 per minute, t = incubation time (24h), and f = factor correcting isotope fractionation during
218 uptake of ^{14}C (1.05).

219

220 **2.4 Chlorophyll-*a* analysis**

221 Seawater samples (250 ml) were filtered onto Whatman GF/F filters at low pressure
222 (<150 mbar), placed in glass vials and frozen in the dark at $-20\ ^\circ\text{C}$. Chlorophyll-*a* was extracted
223 with 5 ml of cold acetone (90%) overnight and determined by the non-acidification method
224 (Welschmeyer, 1994) using a Turner Designs (Trilogy) fluorometer.

225

226 **2.5 Statistical analysis**

227 Pairwise relationships between environmental variables and process rates were
228 evaluated using Pearson correlation coefficients calculated across all individual observations,

229 including all sampled depths (0-100 m) and stations. No prior averaging by depth or profile
230 was applied. Because many variables co-vary with depth and season, these correlations should
231 be interpreted as measures of co-variation rather than independent or causal relationships. Full
232 Pearson correlation statistics (r , r^2 , p -values) are provided in Supplementary Tables S1 and S2.
233 Statistical analyses were performed using Python.

234

235 **3 Results and discussion**

236 **3.1 Physiochemical and biological characteristics of the GoA during summertime**

237 Sampling spanned from late spring (May) to the end of summer (September) within the
238 euphotic zone (0-100 m) of the GoA. Surface temperatures ranged from ~ 25 °C in May to ~ 28
239 °C at the end of summer (September) and declined to ~ 23.5 °C at 100 m during all sampling
240 events (Figure 1A). Photosynthetic active radiation (PAR) levels ranged from ~ 1200 - 1950
241 $\mu\text{mol quanta m}^{-2} \text{ s}^{-1}$ at the surface and decreased exponentially to ~ 10 - 20 $\mu\text{mol quanta m}^{-2} \text{ s}^{-1}$
242 at 100 m (Figure 1B), corresponding to 0.5-1.8% of the surface irradiation levels. The
243 corresponding diffuse attenuation coefficient (K_d) was ~ 0.03 - 0.04 m^{-1} , in agreement with
244 previous observations from the GoA (Dishon et al., 2012; Stambler, 2006) as well as in other
245 oligotrophic regimes (Stambler, 2012). Concentrations of NH_4^+ ranged from undetectable to
246 65 nmol L^{-1} (Figure 1C). The corresponding integrated NH_4^+ inventory (0-100 m) was lowest
247 in May (1.68 $\mu\text{mol m}^{-2}$) and highest in July (~ 4.57 $\mu\text{mol m}^{-2}$) (Table 1). NO_2^- levels were
248 generally low throughout the upper 100 m (from below detection to <20 nmol L^{-1}), except in
249 September when nitrite increased with depth reaching ~ 45 nmol L^{-1} below 40 m (Figure 1D).
250 Vertical NO_2^- profiles suggest active ammonia oxidation below the strongly lit surface waters,
251 especially during September, although we cannot rule out expulsion of NO_2^- by phytoplankton
252 under light limitation (Berube et al., 2023; Collos, 1998). The vertically integrated NO_2^-
253 inventories ranged from 0.79 - 3.39 $\mu\text{mol m}^{-2}$ (Table 1). Surface NO_3^- was also low (<20 nmol
254 L^{-1}) and generally increased with depth, suggesting organic matter regeneration and
255 nitrification during summertime (Figure 1E), and/or that less NO_3^- is assimilated by
256 phytoplankton at deeper depths. The integrated NO_3^- inventory ranged from 2.65 $\mu\text{mol m}^{-2}$ in
257 May and September up to 10.36 $\mu\text{mol m}^{-2}$ in June (Table 1). Collectively, the summertime
258 inorganic N species concentrations in the upper 100 m were low, in agreement with previous
259 reports from the oligotrophic GoA (Mackey et al., 2011; Meeder et al., 2012; Rahav et al.,
260 2015).

261 Chlorophyll-*a* concentrations were low in the surface water (<0.15 $\mu\text{g L}^{-1}$) and
262 gradually increased with depth reaching maximal values in May and June (~ 0.60 $\mu\text{g L}^{-1}$)

263 (Figure 2A). The corresponding integrated chlorophyll-*a* was 26-28 mg m⁻² except in August
 264 where it was 16 mg m⁻² (Table 1). As expected, photosynthesis rates were highest in the surface
 265 water and decreased with depth (Figure 2B), coinciding with the decreasing PAR levels (Figure
 266 1B). Photosynthesis rates decreased from ~10 µg C L⁻¹ d⁻¹ at the surface to below detection at
 267 100 m, except in September when elevated rates were observed throughout the water column,
 268 ranging from ~10 to 25 µg C L⁻¹ d⁻¹ (Figure 2B). The resulting integrated photosynthesis rates
 269 ranged from 242 mg C m⁻² d⁻¹ in August to as high as 1263 mg C m⁻² d⁻¹ in September (Table
 270 1). Despite the fluctuation in photosynthetic rates between months, these values are within the
 271 range previously reported from the GoA (Rahav et al., 2015; Reich et al., 2024; Suggett et al.,
 272 2009).

273 Chemoautotrophic DCF was lower than photosynthesis rates and exhibited no clear
 274 vertical trends (Figure 2C). The surface DCF ranged from ~0.2-0.6 µg C L⁻¹ d⁻¹ to ~0.1-0.9 µg
 275 C L⁻¹ d⁻¹ at 100 m (Figure 2C). The resulting integrated DCF ranged from 17-37 mg C m⁻² d⁻¹,
 276 in agreement with a recent study from the GoA (Reich et al., 2024), corresponding to ~3-10%
 277 of all the total autotrophic activity (photosynthesis and DCF combined). While multiple
 278 microbial metabolisms involve chemoautotrophic carbon fixation, DCF is primarily attributed
 279 to ammonia and nitrite oxidation, as these chemoautotrophic metabolisms are ubiquitous
 280 throughout the oxic water column (Middelburg, 2011; Tang et al., 2023). In general, ammonia
 281 oxidation likely provides energy that supports chemoautotrophic CO₂ assimilation throughout
 282 the euphotic zone. Though less energy efficient, nitrite oxidation also contributes to DCF and
 283 is considered especially relevant near the base of the euphotic zone where NO₂⁻ often
 284 accumulates and reaches a maximum in concentration (Tang et al., 2023).

285

286 **Table 1:** Summary of integrated values (0-100 m) measured in the GoA (N Red Sea) during
 287 summer 2023.

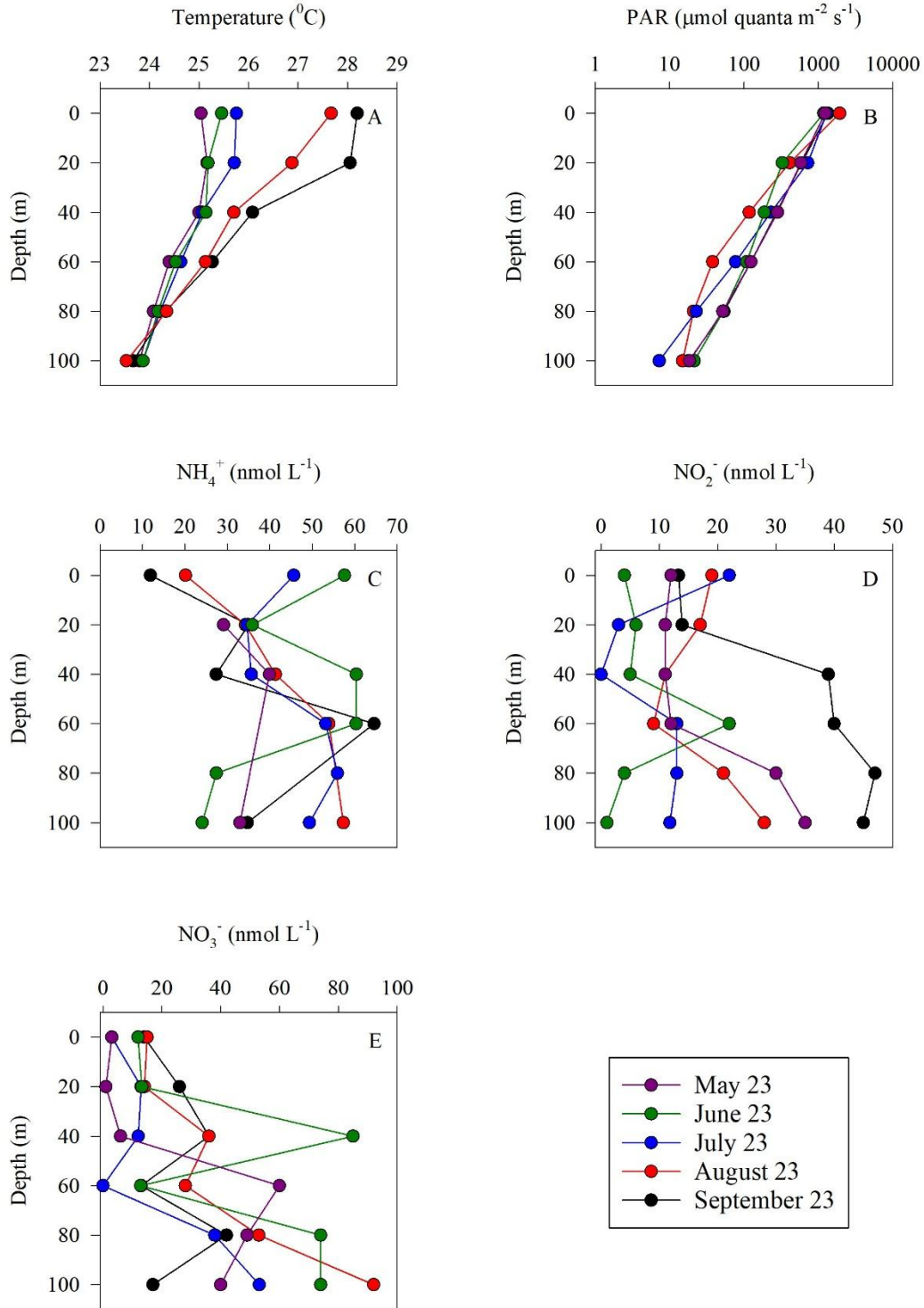
Variable	May 23	June 23	July 23	Aug. 23	Sept. 23
Mixed layer depth (m)*	45	31	21	15	28
NH ₄ ⁺ (µmol m ⁻²)	1.68	4.54	4.57	3.36	2.99
NO ₂ ⁻ (µmol m ⁻²)	1.76	0.79	0.94	1.64	3.39
NO ₃ ⁻ (µmol m ⁻²)	2.76	10.36	6.60	6.13	2.65
Chlorophyll- <i>a</i> (mg m ⁻²)	26	28	26	16	28
Photosynthesis (mg C m ⁻² d ⁻¹)	350	349	302	242	1263
DCF (mg C m ⁻² d ⁻¹)	32	17	35	27	37
NH ₄ ⁺ oxidation (µmol m ⁻² d ⁻¹)	28	48	39	45	56
NO ₂ ⁻ oxidation (µmol m ⁻² d ⁻¹)	24	38	45	39	44
Contribution of NH ₄ ⁺ oxidation to DCF (%)**	0.32	1.02	0.40	0.60	0.54

Contribution of NO_2^- oxidation to DCF (%)*** 0.05 0.13 0.08 0.09 0.07

288 * Calculated from a temperature threshold criterion ($\Delta T = 0.2 \text{ }^\circ\text{C}$ from surface values (de
 289 Boyer Montégut et al., 2004).

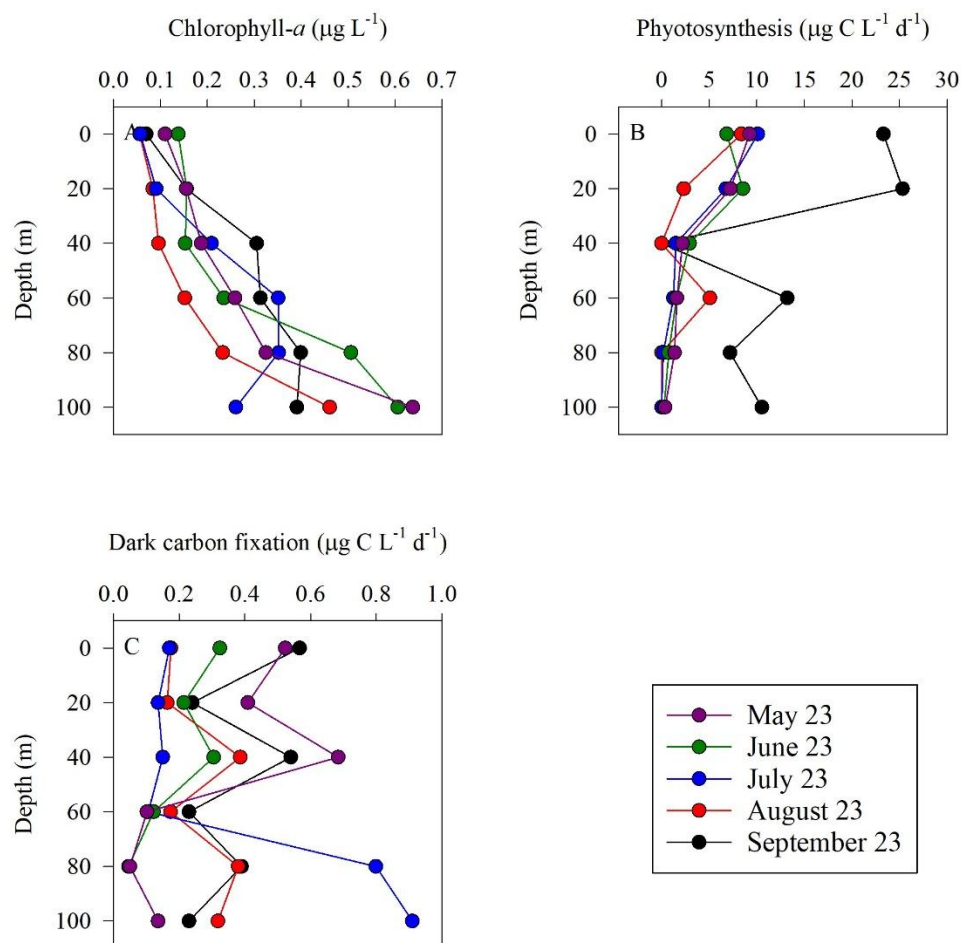
290 **Assuming 0.3 moles of C fixed per mole of NH_4^+ oxidized (Santoro et al., 2010).

291 ***Assuming 0.05 moles of C per mole of NO_2^- oxidized (Beman et al., 2013).



292

293 **Figure 1:** Vertical distribution of temperature (A), PAR (B), NH_4^+ (C), NO_2^- (D) and NO_3^- (E)
 294 in the upper euphotic zone in the GoA, N Red Sea between May and September 2023.



295
 296 **Figure 2:** Vertical distribution of chlorophyll-*a* (A), photosynthesis (B), and dark carbon
 297 fixation (C) in the upper euphotic zone in the GoA, N Red Sea between May and September
 298 2023.

299
 300 **3.2 Ammonia and nitrite oxidation rates**

301 Ammonia and nitrite oxidation rates were generally low throughout the euphotic zone
 302 yet exhibited an increasing trend with depth (Figure 3), consistent with regulation by light
 303 inhibition. Overall, ammonia oxidation was homogeneous in the upper 40 m, ranging from
 304 ~ 0.10 - $0.55 \text{ nmol N L}^{-1} \text{d}^{-1}$. Below this depth rates increased towards the bottom of the euphotic
 305 zone ($\sim 100 \text{ m}$), ranging from ~ 0.26 - $0.83 \text{ nmol N L}^{-1} \text{d}^{-1}$ (Figure 3A,B). Ammonia oxidation
 306 rates often reached a maximum near the base of the euphotic zone (below the 50-100 m layer)
 307 as seen in other studies (reviewed by Tang et al., 2023). In general, these low euphotic zone
 308 ammonia oxidation rates are consistent with light inhibition, given the high PAR of the GoA
 309 during summer (Figure 1B, Wan et al., 2021). Competition of nitrifiers with phytoplankton for

310 NH_4^+ may also result in low ammonia oxidation rates, as has been reported in the surface sunlit
311 North Pacific (Smith et al., 2014). However, the highest integrated ammonia oxidation rate
312 (September, $56 \mu\text{mol m}^{-2} \text{d}^{-1}$) was measured when chlorophyll-*a* levels and primary
313 productivity were also relatively high and similar to springtime when the lowest ammonia
314 oxidation rates were measured (May, $28 \mu\text{mol m}^{-2} \text{d}^{-1}$) (Table 1). Thus, competition between
315 nitrifiers and phytoplankton for NH_4^+ does not appear to play a direct role in the regulation of
316 oxidation rates in our study. That said, the lack of correlation between chlorophyll *a* and
317 ammonia ($R^2=0.003$) does not preclude competition, but instead likely reflects rapid recycling
318 and tight coupling between ammonium production and uptake. Ammonia oxidation rates have
319 also been shown to be influenced by trace metal availability, specifically iron and copper
320 (Martocello and Wankel, 2024; Shafiee et al., 2019, 2021). However, given the close proximity
321 to major deserts, iron is not considered a limiting factor for microbes in the surface water of
322 the GoA (Chen et al., 2008; Torfstein et al., 2017). The limiting factors for ammonia oxidizers
323 in the GoA should be further studied by simulating different nutrients and temperature
324 scenarios with or without amendments of an inhibitor of ammonia monooxygenase to better
325 examine controls on environmental rates (Bayer et al., 2025).

326 During the study period, the mixed layer depth shoaled from ~ 45 m in May to ~ 15 m
327 in August (Table 1), reflecting progressive seasonal stratification. The vertical pattern of
328 ammonia oxidation (Figure 3) suggests that rates remained low throughout the strongly
329 illuminated upper water column, while modest increases at 60–80 m likely reflected reduced
330 light inhibition and/or more favorable conditions for nitrifier activity below the mixed layer.
331 Thus, unlike systems where ammonia oxidation increases sharply below the deep chlorophyll
332 maximum, nitrification in the GoA appears to follow a more gradual depth-related response
333 during stratified conditions.

334 As with ammonia oxidation, rates of nitrite oxidation also increased with depth (Figure
335 3C,D). Nitrite oxidation ranged from 0.14 to 0.70 $\text{nmol L}^{-1} \text{d}^{-1}$ (Figure 3C,D), with highest rates
336 measured over 80-100 m. Integrated nitrite oxidation rates were lowest in spring/early summer
337 ($\sim 24 \mu\text{mol m}^{-2} \text{d}^{-1}$) and increased between June to September ($38\text{-}45 \mu\text{mol m}^{-2} \text{d}^{-1}$) (Table 1).
338 Nitrite oxidation maxima (~ 100 m) were deeper than those of ammonia oxidation (~ 60 m).
339 This vertical offset may reflect differences in substrate supply and the decoupling of ammonia
340 and nitrite oxidation along the water column in addition to differential sensitivity to light (Wan
341 et al., 2021). For example, ammonium supply may be more closely linked to shallower
342 regeneration processes, whereas nitrite can accumulate and persist at greater depths (Travis et
343 al., 2024). At the same time, near-zero ambient NO_2^- or NO_3^- at specific depths and months

344 (e.g., 40 m for ammonia oxidation and 60 m for nitrite oxidation in July; Figure 1) reflects
345 extremely low product pool concentrations, which reduces the total N mass available for IRMS
346 analysis. While this simultaneously reduces dilution of the ^{15}N -labelled product, resulting in
347 elevated atom% enrichment, rate estimates at these depths carry greater analytical uncertainty
348 and should be treated as conservative lower bounds on nitrification activity.

349 Our results demonstrate that ammonia and nitrite oxidation occurring at comparable
350 rates, which is consistent with the typically low concentrations of NO_2^- observed in the GoA
351 during summertime (Figure 1D, Meeder et al., 2012), and consistent with the low net
352 accumulation of NO_2^- resulting from limited decoupling between the two steps of nitrification.
353 Converting photosynthesis to nitrogen demand using Redfield stoichiometry ($\text{C:N} \approx 6.6$)
354 suggests that phytoplankton nitrogen requirements in surface waters may substantially exceed
355 the measured nitrification rates. This implies that regenerated nitrogen, including ammonium,
356 is rapidly consumed, potentially limiting its availability for ammonia-oxidizing
357 microorganisms. However, this inference is based on carbon-derived estimates of
358 phytoplankton demand rather than direct measurements of nitrogen uptake and should therefore
359 be interpreted cautiously. Nevertheless, previous studies indicate that ammonia uptake can
360 greatly exceed nitrification rates in oligotrophic surface waters (Mackey et al., 2011).

361 To assess substrate control, we examined the relationship between NH_4^+ concentration
362 and ammonia oxidation rates across depths. This relationship was weak overall (Pearson,
363 $r \approx 0.30$), whereas rates were more strongly associated with depth ($r \approx 0.75$), indicating a
364 dominant role of depth-related gradients (Figure S1, Table S1). When examined by depth
365 intervals (0-50 m vs. 50-100 m), the NH_4^+ -oxidation relationship was weak in the upper 50 m
366 ($r \approx 0.23$) and stronger >50 m ($r \approx 0.41$) (Figure S1, Table S1). This suggests that rapid recycling
367 and competitive uptake weaken NH_4^+ -oxidation rate coupling in surface waters, whereas
368 reduced light inhibition at depth allows a somewhat greater influence of NH_4^+ . These results
369 are consistent with previous studies showing that nitrification maxima are often decoupled
370 from NH_4^+ peaks and instead reflect depth-dependent ecological structuring (Beman et al.,
371 2012).

372 Note that a key consideration in interpreting the measured rates is the relative magnitude of the
373 $^{15}\text{NH}_4^+$ tracer addition compared to ambient substrate concentrations. In the upper euphotic
374 zone, where NH_4^+ concentrations were often near detection limits (Figure 1), the addition of
375 $\sim 20 \text{ nmol L}^{-1}$ (tracer) represented a substantial enrichment of the available pool. Under such
376 conditions, if ammonia oxidation were strongly substrate-limited, one might expect a
377 measurable stimulation of rates. However, the observed rates remained consistently low across

378 depths and sampling periods (Table 1; Figure 3), even under these ‘enriched’ conditions. This
379 suggests that factors other than immediate substrate availability exert primary control over
380 ammonia oxidation in the upper waters of the GoA. These may include low abundances of
381 ammonia-oxidizing archaea (Aizawa et al., 2023; Smith et al., 2016), strong light inhibition in
382 surface waters (Figure 1B), or physiological constraints associated with oligotrophic adaptation
383 (Yin et al., 2024; Zhou et al., 2024). Rather than indicating the absence of substrate limitation
384 *per se*, our results imply that ammonia oxidation operates under a combination of ecological
385 and environmental constraints that limit its overall contribution to nitrogen cycling in this
386 system. Moreover, the use of 24 h incubations introduce additional uncertainty, as internal
387 recycling of ammonium and microbial interactions may partially decouple measured rates from
388 instantaneous *in situ* conditions. Therefore, the rates reported here are interpreted as
389 conservative estimates of nitrification potential in the upper euphotic zone. Adding to that, in
390 oligotrophic systems, rapid recycling of dissolved inorganic nitrogen can influence both
391 substrate availability (Christie-Oleza et al., 2017) and isotopic enrichment during incubation
392 experiments (Stukel, 2020). Thus, processes such as ammonium regeneration and microbial
393 uptake may dilute the ¹⁵N substrate pool or reduce accumulation of labelled products (Braun et
394 al., 2018). However, we surmise that any such processes, if occurred here, would tend to reduce
395 the apparent isotopic enrichment and thus bias rate estimates toward underestimation. Another
396 possible limitation regards the uncertainty in low nutrient concentrations in the GoA (most
397 notably within the upper mixed layer depth) that may propagate into rate calculations, as
398 substrate concentrations are explicitly included in the rate equations (see equations 1-3).
399 However, such uncertainty affects absolute rate estimates proportionally and does not alter the
400 overall interpretation of low nitrification activity. Accordingly, the reported rates should be
401 considered conservative estimates of nitrification activity over the incubation period. Future
402 work in similar ultra-oligotrophic settings could benefit from newer low-concentration nitrate
403 and nitrite isotope protocols (e.g., Jiang et al., 2026), which explicitly target sub nanomolar N
404 species.

405

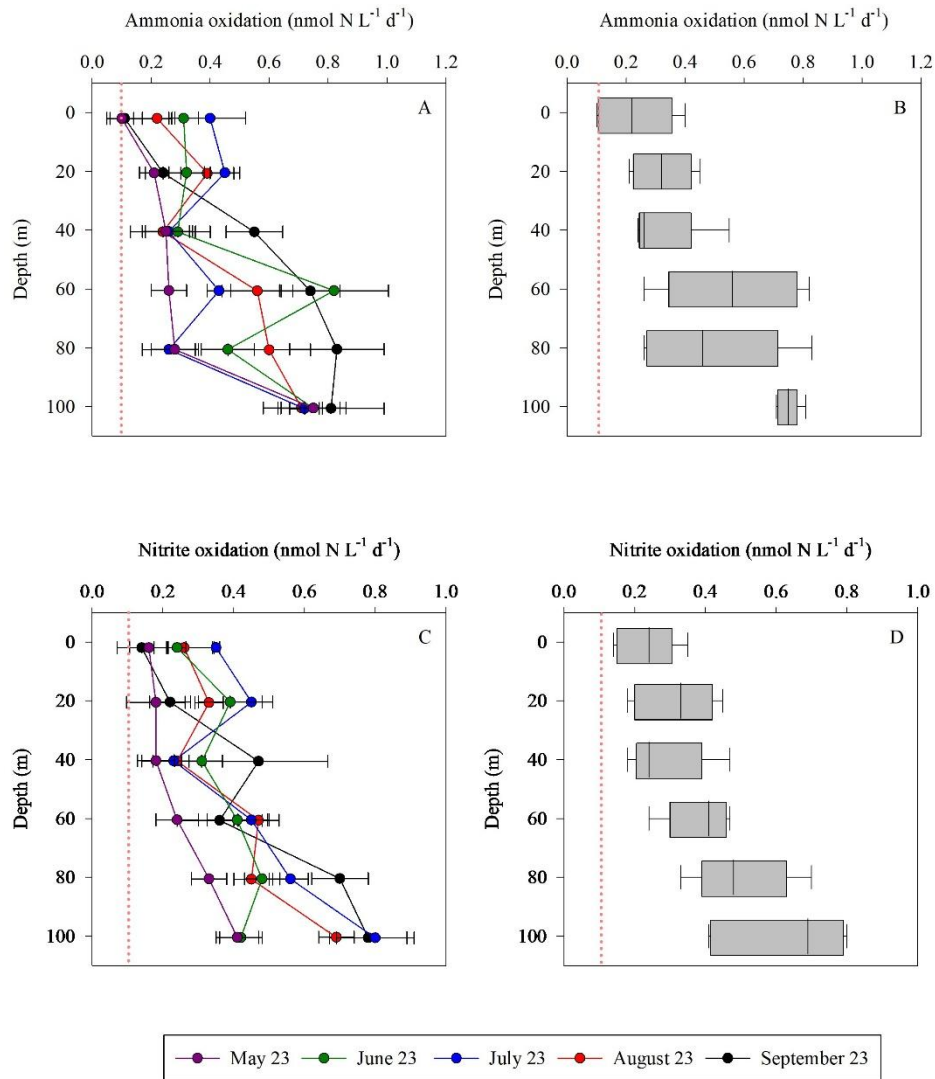
406 **3.3 Contribution of ammonia and nitrite oxidation to DCF**

407 DCF is widely thought to be dominated by ammonia and nitrite oxidation, as these
408 metabolic processes provide energy that, in turn, support chemoautotrophic CO₂ assimilation
409 (Middelburg, 2011), although additional pathways such as urea oxidation by ammonia
410 oxidizers may also contribute (Wan et al., 2024). While other chemoautotrophic metabolisms,
411 such as sulfur oxidation, anammox or methanotrophy also represent important drivers of

412 chemoautotrophy in some environments, these are unlikely to be relevant in the oxic,
413 oligotrophic waters of the GoA. DCF and nitrification are rarely measured simultaneously,
414 which prevents robust assessment of this relationship. Here, we explored DCF under the warm,
415 high-light, nutrient-poor conditions found in the GoA (Figure 1) and investigated how it relates
416 to corresponding rates of nitrification over the euphotic zone. We calculated the contribution
417 of ammonia and nitrite oxidation to DCF assuming 0.3 moles of C fixed per mole of NH_4^+
418 (Santoro et al., 2010). Overall, the depth-integrated contribution of ammonia oxidation to DCF
419 ranged between 0-2%, consistent, yet often lower than reports from other oceanographic
420 settings. For example, ammonia oxidizers contributed only a small fraction to DCF in the
421 eastern tropical Pacific, accounting for <20% of depth-integrated rates (Bayer et al., 2025). The
422 depth-integrated contribution of nitrite oxidation to DCF was negligible, accounting for 0.05-
423 0.13% (Table 1). Thus, ammonia and nitrite oxidation together could account for only ~1% of
424 the DCF, lower than recent estimates from the eastern tropical Pacific (Bayer et al., 2025),
425 though similar to observations in culture experiments with ammonia oxidizers (Bayer et al.,
426 2023). It is notable, however, that relevant conversion factors between moles C fixed per mole
427 of N oxidized in the ocean should be better constrained (and may be site-specific) (Tang et al.,
428 2023), which could alter the calculated contribution discussed here. Nevertheless, we show that
429 ammonia and nitrite oxidation link N recycling with inorganic carbon assimilation in the
430 euphotic zone in the GoA, and while their contribution to total primary production is relatively
431 small, it may sustain part of the microbial metabolism in the nutrient-depleted surface waters
432 of the GoA. Our results suggest that other microbial metabolism processes (e.g., anaplerosis)
433 may also contribute to DCF in the GoA's euphotic zone and should be estimated separately in
434 future studies.

435 DCF in the sunlit ocean should not be interpreted solely as nitrification-driven
436 chemoautotrophy. Even under dark incubation conditions, inorganic carbon fixation may
437 include contributions from phytoplankton-associated dark metabolism, heterotrophic inorganic
438 carbon assimilation, and other microbial pathways (Baltar and Herndl, 2019; Reich et al.,
439 2026). A recent 10-year analysis from the GoA (same study site) showed that DCF is a
440 persistent but variable component of carbon cycling, contributing substantially to total
441 autotrophic carbon fixation (Reich et al., 2024). Therefore, while our data suggests that
442 ammonia and nitrite oxidation contribute only a minor fraction of total DCF, the remaining
443 DCF signal likely reflects multiple unresolved microbial processes (Reich et al., 2025).

444



445

446 **Figure 3:** Vertical distribution of ammonia oxidation (A,B) and nitrite oxidation (C,D) in the
 447 upper euphotic zone in the GoA, N Red Sea between May and September 2023. The Box
 448 Whisker plots sum the data distribution per depth (n=5). The pink dashed line signifies the
 449 detection limit.

450

451 3.4 Environmental divers affecting ammonia and nitrite oxidation

452 Nitrification is known to be affected by PAR, oxygen levels, temperature, nitrogen
 453 substrate availability, pH, as well as by other environmental factors (Ward, 2008). Our results
 454 are consistent overall with previous observations at other sites as both ammonia and nitrite
 455 oxidation rates linearly correlate with most of these environmental variables, either positively
 456 or negatively (Figure 4; Figure S1; Tables S1 and S2). Most notably, ammonia and nitrite
 457 oxidation rates correlated with increasing depth and decreasing PAR level, consistent with
 458 previous reports showing that light inhibit nitrifier growth and nitrification rates (Merbt et al.,
 459 2012; Olsen, 1989; Xu et al., 2019). Temperature correlated negatively with ammonia and

460 nitrite oxidation rates (Figure 4, $r=0.61$, $p<0.01$), likely reflects substrate limitation rather than
461 a direct temperature effect. Previous studies showed that increasing temperature generally
462 stimulates nitrification by simultaneously altering substrate availability and enzyme kinetics
463 (Emerson et al., 1975). As temperature increases, the pKa of the NH_4^+ - NH_3 system decreases,
464 shifting the equilibrium toward NH_3 , the putative substrate of ammonia monooxygenase
465 (Emerson et al., 1975). In parallel, warming enhances enzymatic activity, accelerating the
466 catalytic steps of both ammonia and nitrite oxidation (Zheng et al., 2017, 2020). We surmise
467 that in the stratified GoA, warming strengthened stratification, enhanced photo-inhibition, and
468 thereby increased biological competition for ammonium, thus reducing substrate supply to
469 nitrifiers despite favorable enzyme kinetics, leading to the observed negative correlation
470 between temperature and nitrification. In agreement with this line of thought, substrate
471 availability was positively correlated with ammonia oxidation (NH_4^+ , NO_2^-) and nitrite
472 oxidation (NO_2^- , NO_3^-), highlighting the substrate-dependent nature of nitrification.
473 Alternatively, these relationships may reflect co-variation with depth and associated
474 environmental gradients, rather than direct substrate control alone (discussed below). Ammonia
475 oxidation requires NH_4^+ or NH_3 as the electron donor, while nitrite oxidation depends on NO_2^-
476 availability. Elevated ambient concentrations of these substrates make them more available to
477 nitrifying enzymes, resulting in higher reaction rates until enzymatic saturation or co-limitation
478 with other nutrients are reached (e.g., vitamins and other co-factors, PO_4^+). In oligotrophic
479 systems such as the GoA, where ambient NH_4^+ and NO_2^- concentrations are exceptionally low,
480 even small pulses of reduced or intermediate nitrogen (e.g., from organic matter
481 remineralization, mixing, or atmospheric deposition) may trigger an increase in nitrification
482 rates.

483 Nitrification is generally expected to show a negative relationship with chlorophyll-*a*
484 in surface waters, where phytoplankton may compete with nitrifiers for reduced nitrogen
485 species. Consequently, most studies report suppressed ammonia and nitrite oxidation rates near
486 the surface and enhanced rates below the chlorophyll maximum once light levels decrease and
487 substrate regeneration through organic matter remineralization becomes more important
488 (Beman et al., 2013; Yool et al., 2007). Here, however, we observed a positive correlation
489 between chlorophyll-*a* and ammonia or nitrite oxidation (as well as with photosynthesis,
490 although not significantly). This pattern likely reflects conditions near the deep chlorophyll
491 maximum (~80-100 m), where chlorophyll *a* is elevated due to photo-acclimation under low
492 light conditions rather than strictly higher biomass (Cornec et al., 2021; Fennel and Boss, 2003;
493 Scofield et al., 2020). In these depths, reduced irradiance and enhanced organic matter turnover

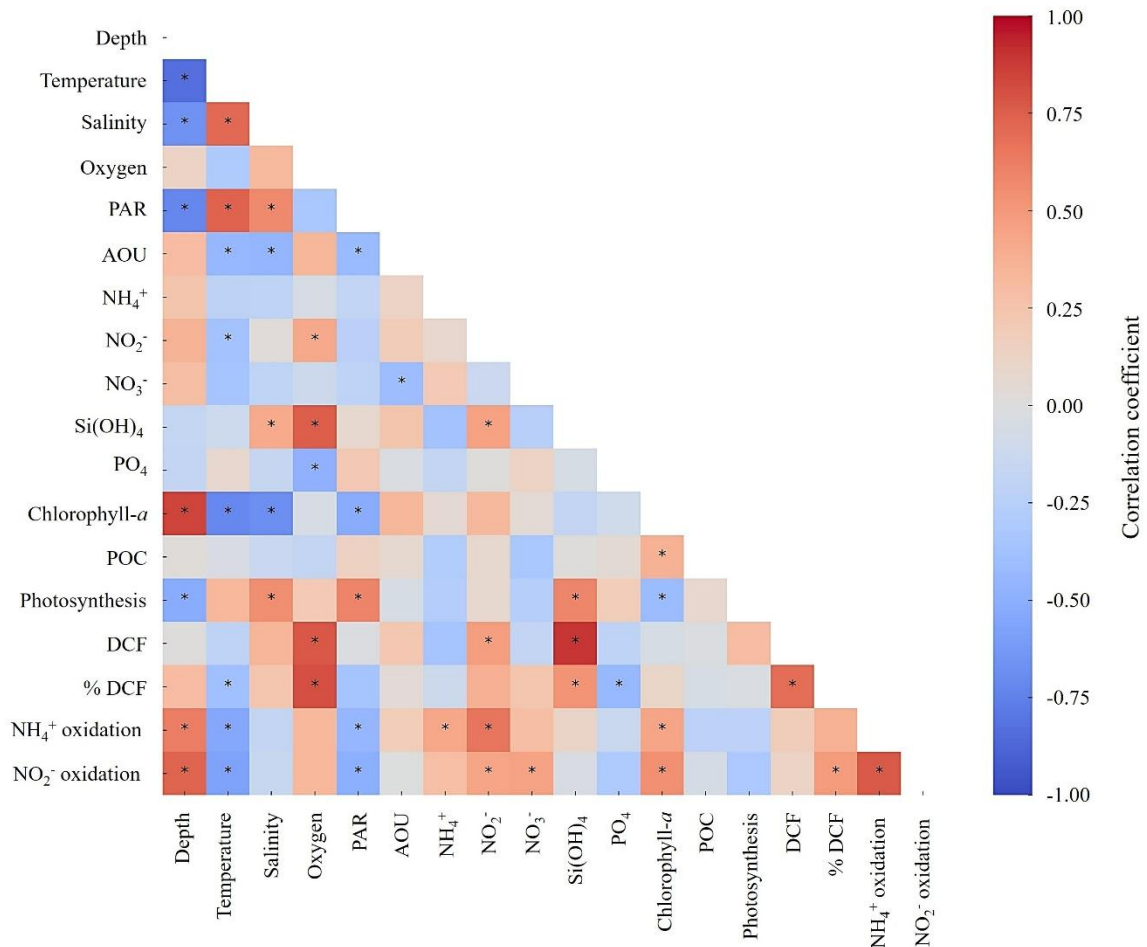
494 may promote ammonium regeneration, providing substrate that supports nitrification. These
495 findings suggest that the expected negative coupling at the surface is offset by strong
496 regeneration and oxidation processes near the deep chlorophyll maxima, resulting in an overall
497 positive relationship when integrated across the euphotic zone.

498 We expected that ammonia and nitrite oxidation would show a significant correlation
499 with DCF (see discussion above). Nevertheless, although both ammonia and nitrite oxidation
500 were positively coupled with DCF ($r=0.49$ and 0.17 , respectively), the correlations were not
501 statistically significant ($p>0.05$) and is in line with the overall low contribution of these
502 processes to DCF (discussion above and see Table 1). This suggests that additional pathways
503 such as anaplerotic processes may contribute to DCF (Dijkhuizen and Harder, 1984; Erb, 2011),
504 as well as other chemoautotrophic metabolisms beyond nitrification such as urea oxidation,
505 sulfur oxidation and iron oxidation (Arandia-Gorostidi et al., 2024; Dang and Chen, 2017),
506 while the contribution of ammonia and nitrite oxidation to total DCF is low (Table 1).

507 We note that correlation analysis should be interpreted with caution. Many parameters
508 considered here co-vary with depth (e.g., PAR, chlorophyll-*a*) and seasonal stratification
509 (mixed layer depth), which can produce strong apparent relationships without implying direct
510 mechanistic coupling. Furthermore, as the dataset is restricted to the upper 100 m, it does not
511 capture the full vertical structure of nitrification, including deeper maxima often observed
512 below the deep chlorophyll maximum. Accordingly, these correlations primarily reflect
513 processes operating within the upper euphotic zone and should not be extrapolated beyond this
514 depth range. Lastly, while variations in ammonia oxidation rates broadly co-occurred with
515 changes in primary production and chlorophyll *a*, these relationships should be interpreted with
516 caution. In this study, phytoplankton activity was assessed using carbon-based proxies, and no
517 direct measurements of nitrogen uptake or community composition were conducted. Therefore,
518 any inferred coupling between phytoplankton dynamics and nitrification remains indirect. The
519 observed patterns are consistent with the expectation that phytoplankton influence the
520 availability and cycling of regenerated nitrogen, but do not allow us to disentangle the relative
521 roles of substrate competition, regeneration, or microbial community structure. Future studies
522 that combine measurements of phytoplankton nitrogen demand, ammonium regeneration, and
523 nitrifier abundance and activity will be required to directly resolve these interactions in
524 oligotrophic systems.

525

526



527

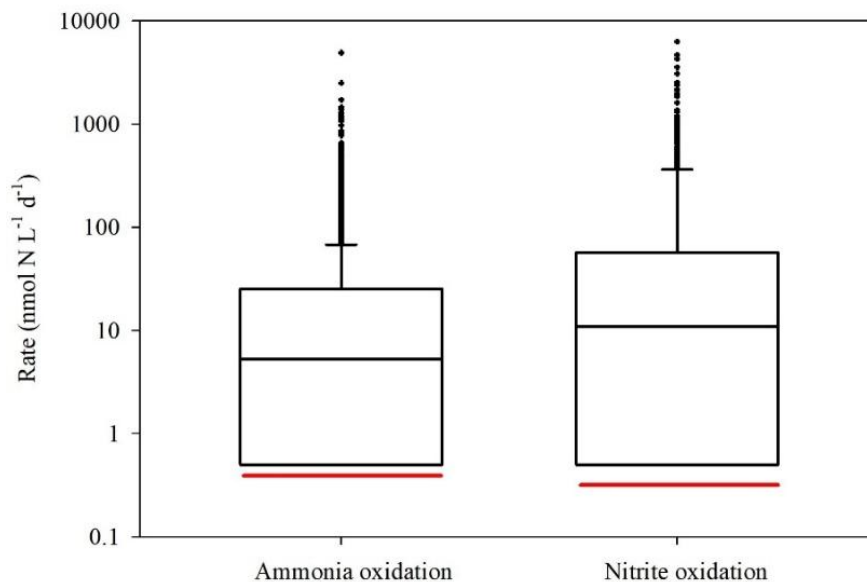
528 **Figure 4:** A heatmap showing Pearson correlation coefficients among measured environmental
 529 parameters and biogeochemical rates. Color shading indicates the strength and direction of the
 530 correlation. Asterisks denote statistically significant correlations ($p < 0.05$). Full descriptive
 531 statistics for the correlations are provided in the Supplementary Tables S1 and S2.

532

533 4 Conclusions

534 Globally, ammonia and nitrite oxidation rates in the euphotic zone span several orders
 535 of magnitude across offshore oceanic environments (Tang et al., 2023, Figure 5). The rates we
 536 measured in the GoA during summer fall below the global median (i.e., the red vs. black lines
 537 in Figure 5). The reason for the low rates in GoA is attributed to the low substrate availability
 538 during summertime (Figure 1C-E) but likely reflect a combination of environmental and
 539 ecological constraints rather than a single controlling factor. For example, the combination of
 540 high light intensity (Figure 1B) and penetration (i.e., $K_d \approx 0.04 \text{ m}^{-1}$) and enhanced stratification
 541 (Figure 1A) can further suppress nitrifier activity, either through photoinhibition of ammonia
 542 monooxygenase and/or by pushing microbial communities closer to their thermal tolerance

543 limits. Moreover, the absence of measurements of nitrifier abundance preclude us from
544 distinguishing whether low bulk rates reflect low population size or potentially high per-cell
545 activity.



546
547 **Figure 5:** A literature compilation of reported euphotic zone’s ammonia oxidation and nitrite
548 oxidation recently reviewed Tang et al., (2023) and this study. The black line inside the boxes
549 shows the median value of all studies considered, while the red line indicates the median values
550 measured in the GoA during this study. Data include only offshore euphotic-zone
551 measurements as defined in the original studies. We note that the depth and definition of the
552 euphotic zone vary among regions, which may contribute to variability in reported rates.
553

554 Additionally, while our results suggest a potential linkage between phytoplankton
555 activity and nitrogen cycling, this inference is based on carbon-derived proxies (primary
556 production and chlorophyll-*a*) rather than direct measurements of species-specific nitrogen
557 uptake or microbial community composition using genetic markers. Resolving this coupling
558 will require future studies that simultaneously quantify phytoplankton nitrogen demand,
559 ammonium regeneration, and nitrifier abundance and activity.

560 Future studies should focus on resolving the temporal and spatial variability of
561 nitrification rates and nitrifier communities in the context of ongoing climate change. This is
562 especially true for the GoA that experience rapid warming and ocean acidification. Long-term
563 time series and diel-scale observations are needed to capture seasonal, interannual, and daily
564 dynamics, particularly in relation to stratification, warming, and nutrient supply. Advanced
565 molecular approaches such as metagenomics, metatranscriptomics, and single-cell tools should
566 be applied to link community composition and functional potential with *in-situ* rate

567 measurements. Parallel measurements of trace metals will be essential to assess their role as
568 cofactors or inhibitors of key enzymes in ammonia and nitrite oxidation. Furthermore, the
569 contribution of nitrification to DCF appears to be limited, suggesting that additional microbial
570 pathways contribute to inorganic carbon fixation in this system. Constraining these
571 contributions will require future studies that integrate rate measurements with microbial
572 community and metabolic analyses to better resolve the sources of DCF in oligotrophic waters.
573 Ultimately, combining high-resolution field observations with targeted manipulations and
574 modelling will improve our ability to predict how nitrification responds to environmental
575 change and contributes to current and future ocean nitrogen cycling.

576 *Data availability.* All the data is presented in the graphs/table/text and will be made available
577 in excel format upon request.

578 *Author contributions.* Conceptualized and conducted the field measurements; ER. Data
579 curation, formal analysis, and visualization; ER, SDW and AP. The paper was prepared by ER,
580 SDW and AP.

581 *Competing interests.* The contact author has declared that none of the authors has any
582 competing interests.

583 *Acknowledgments.* The authors thank the personnel in the Inter University Institute for Marine
584 Sciences in Eilat (IUI). This paper was supported by a grant from the Middle East Regional
585 Cooperation (MERC) (M39-011) to ER and AP. We also thank the two anonymous reviewers
586 for their constructive comments, which helped to significantly improve and refine the
587 manuscript.

588 **References**

589 Aizawa, A., Watanabe, Y., Hashioka, K., Kadoya, A., Suzuki, S., Yoshimura, T., and Kudo,
590 I.: Contribution of ammonium oxidizing archaea and bacteria to intensive nitrification during
591 summer in Mutsu Bay, Japan, *Reg. Stud. Mar. Sci.*, 63, 102984,
592 <https://doi.org/https://doi.org/10.1016/j.rsma.2023.102984>, 2023.

593 Arandia-Gorostidi, N., Jaffe, A. L., Parada, A. E., Kapili, B. J., Casciotti, K. L., Salcedo, R.
594 S. R., Baumas, C. M. J., and Dekas, A. E.: Urea assimilation and oxidation support activity of
595 phylogenetically diverse microbial communities of the dark ocean, *ISME J.*, 18,
596 <https://doi.org/10.1093/ismejo/wrae230>, 2024.

597 Baltar, F. and Herndl, G.: Is dark carbon fixation relevant for oceanic primary production
598 estimates?, *Biogeosciences Discuss.*, 1–12, <https://doi.org/10.5194/bg-2019-223>, 2019.

599 Bayer, B., McBeain, K., Carlson, C. A., and Santoro, A. E.: Carbon content, carbon fixation
600 yield and dissolved organic carbon release from diverse marine nitrifiers, *Limnol. Oceanogr.*,
601 68, 84–96, <https://doi.org/https://doi.org/10.1002/lno.12252>, 2023.

602 Bayer, B., Kitzinger, K., Paul, N. L., Albers, J. B., Saito, M. A., Wagner, M., Carlson, C. A.,
603 and Santoro, A. E.: Minor contribution of ammonia oxidizers to inorganic carbon fixation in
604 the ocean, *Nat. Geosci.*, 18, 1144–1151, <https://doi.org/10.1038/s41561-025-01798-x>, 2025.

605 Beman, J. M., Chow, C.-E., King, A. L., Feng, Y., Fuhrman, J. A., Andersson, A., Bates, N.
606 R., Popp, B. N., and Hutchins, D. A.: Global declines in oceanic nitrification rates as a
607 consequence of ocean acidification, *Proc. Natl. Acad. Sci.*, 108, 208–213,
608 <https://doi.org/10.1073/pnas.1011053108>, 2011.

609 Beman, J. M., Leilei Shih, J., and Popp, B. N.: Nitrite oxidation in the upper water column
610 and oxygen minimum zone of the eastern tropical North Pacific Ocean, *ISME J.*, 7, 2192–
611 2205, <https://doi.org/10.1038/ismej.2013.96>, 2013.

612 Berube, P. M., J., O. T., Anna, R., Trent, L., and W., C. S.: Production and cross-feeding of
613 nitrite within *Prochlorococcus* populations, *MBio*, 14, e01236-23,
614 <https://doi.org/10.1128/mbio.01236-23>, 2023.

615 de Boyer Montégut, C., Madec, G., Fischer, A. S., Lazar, A., and Iudicone, D.: Mixed layer
616 depth over the global ocean: An examination of profile data and a profile-based climatology,
617 *J. Geophys. Res. Ocean.*, 109, C12003, <https://doi.org/https://doi.org/10.1029/2004JC002378>,
618 2004.

619 Braun, J., Mooshammer, M., Wanek, W., Prommer, J., Walker, T. W. N., Rütting, T., and
620 Richter, A.: Full ¹⁵N tracer accounting to revisit major assumptions of ¹⁵N isotope pool
621 dilution approaches for gross nitrogen mineralization, *Soil Biol. Biochem.*, 117, 16–26,
622 <https://doi.org/https://doi.org/10.1016/j.soilbio.2017.11.005>, 2018.

623 Bristow, L. A., Sarode, N., Cartee, J., Caro-Quintero, A., Thamdrup, B., and Stewart, F. J.:
624 Biogeochemical and metagenomic analysis of nitrite accumulation in the Gulf of Mexico
625 hypoxic zone, *Limnol. Oceanogr.*, 60, 1733–1750,
626 <https://doi.org/https://doi.org/10.1002/lno.10130>, 2015.

627 Buchwald, C., Homola, K., Spivack, A. J., Estes, E. R., Murray, R. W., and Wankel, S. D.:
628 Isotopic constraints on nitrogen transformation rates in the deep sedimentary marine
629 biosphere, *Global Biogeochem. Cycles*, 32, 1688–1702,
630 <https://doi.org/https://doi.org/10.1029/2018GB005948>, 2018.

631 Casciotti, K. L., Sigman, D. M., Hastings, M. G., Böhlke, J. K., and Hilkert, A.:
632 Measurement of the oxygen isotopic composition of nitrate in seawater and freshwater using
633 the denitrifier method., *Anal. Chem.*, 74, 4905–4912, <https://doi.org/10.1021/ac020113w>,
634 2002.

635 Chen, Y., Paytan, A., Chase, Z., Measures, C., Beck, A. J., Sañudo-Wilhelmy, S. A., and
636 Post, A. F.: Sources and fluxes of atmospheric trace elements to the Gulf of Aqaba, Red Sea,
637 *J. Geophys. Res. Atmos.*, 113, 1–13, <https://doi.org/10.1029/2007JD009110>, 2008.

638 Christie-Oleza, J. A., Sousoni, D., Lloyd, M., Armengaud, J., and Scanlan, D. J.: Nutrient
639 recycling facilitates long-term stability of marine microbial phototroph-heterotroph
640 interactions, *Nat. Microbiol.*, 2, 17100, <https://doi.org/10.1038/nmicrobiol.2017.100>, 2017.

641 Clark, D. R., Rees, A. P., and Joint, I.: Ammonium regeneration and nitrification rates in the

642 oligotrophic Atlantic Ocean: Implications for new production estimates, *Limnol. Oceanogr.*,
643 53, 52–62, <https://doi.org/https://doi.org/10.4319/lo.2008.53.1.0052>, 2008.

644 Clark, D. R., Rees, A. P., Ferrera, C. M., Al-moosawi, L., Somerfield, P. J., Harris, C.,
645 Quartly, G. D., Goult, S., Tarran, G., and Lessin, G.: Nitrite regeneration in the oligotrophic
646 Atlantic Ocean, *Biogeosciences*, 19, 1355–1376, [https://doi.org/https://doi.org/10.5194/bg-](https://doi.org/https://doi.org/10.5194/bg-19-1355-2022)
647 19-1355-2022, 2022.

648 Collos, Y.: Nitrate uptake, nitrite release and uptake, and new production estimates, *Mar.*
649 *Ecol. Prog. Ser.*, 171, 293–301, 1998.

650 Cornec, M., Claustre, H., Mignot, A., Guidi, L., Lacour, L., Poteau, A., D’Ortenzio, F.,
651 Gentili, B., and Schmechtig, C.: Deep chlorophyll maxima in the global ocean: occurrences,
652 drivers and characteristics, *Glob. Biochem. cycles*, 35, e2020GB006759,
653 <https://doi.org/10.1029/2020GB006759>, 2021.

654 Daims, H., Lebedeva, E. V, Pjevac, P., Han, P., Herbold, C., Albertsen, M., Jehmlich, N.,
655 Palatinszky, M., Vierheilig, J., Bulaev, A., Kirkegaard, R. H., von Bergen, M., Rattei, T.,
656 Bendinger, B., Nielsen, P. H., and Wagner, M.: Complete nitrification by *Nitrospira* bacteria,
657 *Nature*, 528, 504–509, <https://doi.org/10.1038/nature16461>, 2015.

658 Dang, H. and Chen, C.-T. A.: Ecological energetic perspectives on responses of nitrogen-
659 transforming chemolithoautotrophic microbiota to changes in the marine environment, *Front.*
660 *Microbiol.*, 8, 1246, <https://doi.org/10.3389/fmicb.2017.01246>, 2017.

661 Dijkhuizen, L. and Harder, W.: Current views on the regulation of autotrophic carbon dioxide
662 fixation via the Calvin cycle in bacteria, *Antonie Van Leeuwenhoek*, 50, 473–487, 1984.

663 Dishon, G., Dubinsky, Z., Caras, T., Rahav, E., Bar-Zeev, E., Tzuber, Y., and Iluz, D.:
664 Optical habitats of ultraphytoplankton groups in the Gulf of Eilat (Aqaba), Northern Red Sea,
665 *Int. J. Remote Sens.*, 33, 2683–2705, <https://doi.org/10.1080/01431161.2011.619209>, 2012.

666 Dodds, W. K. and Jones, R. D.: Potential rates of nitrification and denitrification in an
667 oligotrophic freshwater sediment system, *Microb. Ecol.*, 14, 91–100, 1987.

668 Emerson, K., Russo, R. C., Lund, R. E., and Thurston, R. V: Aqueous ammonia equilibrium
669 calculations: effect of pH and temperature, *J. Fish. Res. Board Canada*, 32, 2379–2383,
670 <https://doi.org/10.1139/f75-274>, 1975.

671 Eppley, R. W. and Peterson, B. J.: Particulate organic matter flux and planktonic new
672 production in the deep ocean, *Nature*, 282, 677–680, <https://doi.org/10.1038/282677a0>, 1979.

673 Erb, T. J.: Carboxylases in natural and synthetic microbial pathways,
674 <https://doi.org/10.1128/AEM.05702-11>, December 2011.

675 Fawcett, S. E., Lomas, M. W., Casey, J. R., Ward, B. B., and Sigman, D. M.: Assimilation of
676 upwelled nitrate by small eukaryotes in the Sargasso Sea, *Nat. Geosci.*, 4, 717–722,
677 <https://doi.org/10.1038/ngeo1265>, 2011.

678 Fei, X., Jian-Gong, W., Ting, Z., Bin, Z., Sung-Keun, R., and Zhe-Xue, Q.: Ubiquity and
679 diversity of complete ammonia oxidizers (Comammox), *Appl. Environ. Microbiol.*, 84,
680 e01390-18, <https://doi.org/10.1128/AEM.01390-18>, 2018.

681 Fennel, K. and Boss, E.: Subsurface maxima of phytoplankton and chlorophyll: Steady-state
682 solutions from a simple model, *Limnol. Oceanogr.*, 48, 1521–1534,
683 <https://doi.org/https://doi.org/10.4319/lo.2003.48.4.1521>, 2003.

684 Francis, C. A., Roberts, K. J., Beman, J. M., Santoro, A. E., and Oakley, B. B.: Ubiquity and
685 diversity of ammonia-oxidizing archaea in water columns and sediments of the ocean, *Proc.*
686 *Natl. Acad. Sci.*, 102, 14683–14688, <https://doi.org/10.1073/pnas.0506625102>, 2005.

687 Fuller, N. J., West, N. J., Marie, D., Yallop, M., Rivlin, T., Post, A. F., Interuniversity, T.,
688 Sciences, M., Beach, C., and Scanlan, D. J.: Dynamics of community structure and phosphate
689 status of picocyanobacterial populations in the Gulf of Aqaba , *Red Sea*, 50, 363–375, 2005.

690 Granger, J. and Sigman, D. M.: Removal of nitrite with sulfamic acid for nitrate N and O
691 isotope analysis with the denitrifier method, *Rapid Commun. Mass Spectrom.*, 23, 3753–
692 3762, <https://doi.org/10.1002/rcm.4307>, 2009.

693 Grasshoff, K., Kremling, K., and Ehrhardt, M.: *Methods of seawater analysis*, 3rd ed., edited
694 by: Kremling, K., Ehrenreich, I. M., and Grasshoff, K., Wiley, New York, 632 pp., 1999.

695 Henriksen, K. and Kemp, W. M.: Nitrification in estuarine and coastal marine sediments, in:
696 *Nitrogen Cycling in Coastal Marine Environments*, edited by: Blackburn, T. . and Sorensen,
697 J., John Wiley & Sons, Ltd, 207–249, 1988.

698 Herbert, R. A.: Nitrogen cycling in coastal marine ecosystems, *FEMS Microbiol. Rev.*, 23,
699 563–590, <https://doi.org/10.1111/j.1574-6976.1999.tb00414.x>, 1999.

700 Holms, R. ., Aminot, A., K erouel, R., Hooker, B. ., and Peterson, B. .: A simple and precise
701 method for measuring ammonium in marine and freshwater ecosystems, *Can. Data Rep. Fish.*
702 *Aquat. Sci.*, 56, 1801–1808, <https://doi.org/10.1139/cjfas-56-10-1801>, 1999.

703 Jiang, M., Koba, K., Ono, M., and Hayashi, K.: Improved isotopic analysis of low-
704 concentration freshwater nitrite by anion-exchange resin enrichment and azide reduction,
705 *Anal. Chem.*, 98, 2956–2967, <https://doi.org/10.1021/acs.analchem.5c05937>, 2026.

706 van Kessel, M. A. H. J., Speth, D. R., Albertsen, M., Nielsen, P. H., Op den Camp, H. J. M.,
707 Kartal, B., Jetten, M. S. M., and L ucker, S.: Complete nitrification by a single
708 microorganism, *Nature*, 528, 555–559, <https://doi.org/10.1038/nature16459>, 2015.

709 Mackey, K. R. M., Labiosa, R. G., Calhoun, M., Street, J. H., Post, A. F., and Paytan, A.:
710 Phosphorus availability, phytoplankton community dynamics, and taxon-specific phosphorus
711 status in the Gulf of Aqaba, Red Sea, *Limnol. Oceanogr.*, 52, 873–885,
712 <https://doi.org/10.4319/lo.2007.52.2.0873>, 2007.

713 Mackey, K. R. M., Bristow, L., Parks, D. R., Altabet, M. A., Post, A. F., and Paytan, A.: The
714 influence of light on nitrogen cycling and the primary nitrite maximum in a seasonally
715 stratified sea, *Prog. Oceanogr.*, 91, 545–560,
716 <https://doi.org/https://doi.org/10.1016/j.pocean.2011.09.001>, 2011.

717 Martocello, D. E. and Wankel, S. D.: Physiological influence of Fe and Cu availability on
718 nitrogen isotope fractionation during ammonia oxidation, *Environ. Sci. Technol.*, 58, 421–
719 431, <https://doi.org/10.1021/acs.est.3c05964>, 2024.

720 McIlvin, M. R. and Casciotti, K. L.: Technical updates to the bacterial method for nitrate
721 isotopic analyses, *Anal. Chem.*, 83, 1850–1856, <https://doi.org/10.1021/ac1028984>, 2011.

722 Mduyana, M., Thomalla, S. J., Philibert, R., Ward, B. B., and Fawcett, S. E.: The seasonal
723 cycle of nitrogen uptake and nitrification in the Atlantic sector of the Southern Ocean, *Global*
724 *Biogeochem. Cycles*, 34, e2019GB006363,
725 <https://doi.org/https://doi.org/10.1029/2019GB006363>, 2020.

- 726 Meeder, E., MacKey, K. R. M., Paytan, A., Shaked, Y., Iluz, D., Stambler, N., Rivlin, T.,
727 Post, A. F., and Lazar, B.: Nitrite dynamics in the open ocean-clues from seasonal and
728 diurnal variations, *Mar. Ecol. Prog. Ser.*, 453, 11–26, <https://doi.org/10.3354/meps09525>,
729 2012.
- 730 Merbt, S. N., Stahl, D. A., Casamayor, E. O., Martí, E., Nicol, G. W., and Prosser, J. I.:
731 Differential photoinhibition of bacterial and archaeal ammonia oxidation, *FEMS Microbiol.*
732 *Let.*, 327, 41–46, <https://doi.org/10.1111/j.1574-6968.2011.02457.x>, 2012.
- 733 Michael Beman, J., Popp, B. N., and Alford, S. E.: Quantification of ammonia oxidation rates
734 and ammonia-oxidizing archaea and bacteria at high resolution in the Gulf of California and
735 eastern tropical North Pacific Ocean, *Limnol. Oceanogr.*, 57, 711–726,
736 <https://doi.org/https://doi.org/10.4319/lo.2012.57.3.0711>, 2012.
- 737 Middelburg, J. J.: Chemoautotrophy in the ocean, *Geophys. Res. Lett.*, 38, 94–97,
738 <https://doi.org/10.1029/2011GL049725>, 2011.
- 739 Mincer, T. J., Church, M. J., Taylor, L. T., Preston, C., Karl, D. M., and DeLong, E. F.:
740 Quantitative distribution of presumptive archaeal and bacterial nitrifiers in Monterey Bay and
741 the North Pacific Subtropical Gyre, *Environ. Microbiol.*, 9, 1162–1175,
742 <https://doi.org/https://doi.org/10.1111/j.1462-2920.2007.01239.x>, 2007.
- 743 Olsen, R.: Differential photoinhibition of marine nitrifying bacteria: a possible mechanism
744 for the formation of the primary nitrite maximum, *J. Mar. Syst.*, 31, 227–238, 1989.
- 745 Pachiadaki, M. G., Sintes, E., Bergauer, K., Brown, J. M., Record, N. R., Swan, B. K.,
746 Mathyer, M. E., Hallam, S. J., Lopez-Garcia, P., Takaki, Y., Nunoura, T., Woyke, T., Herndl,
747 G. J., and Stepanauskas, R.: Major role of nitrite-oxidizing bacteria in dark ocean carbon
748 fixation, *Science (80-.)*, 358, 1046–1051, <https://doi.org/10.1126/science.aan8260>, 2017.
- 749 Rahav, E., Herut, B., Mulholland, M. R., Belkin, N., Elifantz, H., and Berman-Frank, I.:
750 Heterotrophic and autotrophic contribution to dinitrogen fixation in the Gulf of Aqaba, *Mar.*
751 *Ecol. Prog. Ser.*, 522, 67–77, <https://doi.org/10.3354/meps11143>, 2015.
- 752 Reich, T., Belkin, N., Sisma-Ventura, G., Berman-Frank, I., and Rahav, E.: Significant dark
753 inorganic carbon fixation in the euphotic zone of an oligotrophic sea, *Limnol. Oceanogr.*,
754 9999, 1–14, <https://doi.org/10.1002/lno.12560>, 2024.
- 755 Reich, T., Belkin, N., Sisma-Ventura, G., Hauzer, H., Rubin-Blum, M., Berman-Frank, I.,
756 and Rahav, E.: Contribution of dark inorganic carbon fixation to bacterial carbon demand in
757 the oligotrophic Southeastern Mediterranean Sea, *Ocean Sci.*, 21, 3055–3067,
758 <https://doi.org/10.5194/os-21-3055-2025>, 2025.
- 759 Reich, T., Belkin, N., Sisma-ventura, G., Hauzer, H., Berman-frank, I., and Rahav, E.: Does
760 oligotrophy favor chemoautotrophy over photoautotrophy ?, *Prog. Oceanogr.*, 241, 103633,
761 <https://doi.org/10.1016/j.pcean.2025.103633>, 2026.
- 762 Santoro, A. E., Casciotti, K. L., and Francis, C. A.: Activity, abundance and diversity of
763 nitrifying archaea and bacteria in the central California current, *Environ. Microbiol.*, 12,
764 1989–2006, <https://doi.org/https://doi.org/10.1111/j.1462-2920.2010.02205.x>, 2010.
- 765 Scofield, A. E., Watkins, J. M., Osantowski, E., and Rudstam, L. G.: Deep chlorophyll
766 maxima across a trophic state gradient: A case study in the Laurentian Great Lakes., *Limnol.*
767 *Oceanogr.*, 65, 2460–2484, <https://doi.org/10.1002/lno.11464>, 2020.
- 768 Shafiee, R. T., Snow, J. T., Zhang, Q., and Rickaby, R. E. M.: Iron requirements and uptake

769 strategies of the globally abundant marine ammonia-oxidising archaeon, *Nitrosopumilus*
770 *maritimus* SCM1, *ISME J.*, 13, 2295–2305, <https://doi.org/10.1038/s41396-019-0434-8>,
771 2019.

772 Shafiee, R. T., Diver, P. J., Snow, J. T., Zhang, Q., and Rickaby, R. E. M.: Marine ammonia-
773 oxidising archaea and bacteria occupy distinct iron and copper niches, *ISME Commun.*, 1, 1,
774 <https://doi.org/10.1038/s43705-021-00001-7>, 2021.

775 Shiozaki, T., Ijichi, M., Fujiwara, A., Makabe, A., Nishino, S., Yoshikawa, C., and Harada,
776 N.: Factors regulating nitrification in the Arctic Ocean: potential impact of sea ice reduction
777 and ocean acidification, *Global Biogeochem. Cycles*, 33, 1085–1099,
778 <https://doi.org/https://doi.org/10.1029/2018GB006068>, 2019.

779 Sigman, D. M., Casciotti, K. L., Andreani, M., Barford, C., Galanter, M., and Böhlke, J. K.:
780 A bacterial method for the nitrogen isotopic analysis of nitrate in seawater and freshwater,
781 *Anal. Chem.*, 73, 4145–4153, <https://doi.org/10.1021/ac010088e>, 2001.

782 Smith, J. M., Damashek, J., Chavez, F. P., and Francis, C. A.: Factors influencing
783 nitrification rates and the abundance and transcriptional activity of ammonia-oxidizing
784 microorganisms in the dark northeast Pacific Ocean, *Limnol. Oceanogr.*, 61, 596–609,
785 <https://doi.org/https://doi.org/10.1002/lno.10235>, 2016.

786 Stambler, N.: Light and picophytoplankton in the Gulf of Eilat (Aqaba), *J. Geophys. Res.*,
787 111, C11009, 2006.

788 Stambler, N.: Underwater light field of the Mediterranean Sea, in: *Life in the Mediterranean*
789 *Sea: A Look at Habitat Changes*, edited by: Stambler, N., Nova Science Publishers, 1–739,
790 2012.

791 Steemann-Nielsen, E.: The use of radioactive carbon (¹⁴C) for measuring organic production
792 in the sea, *J. des Cons. Int. Pour Explor. la Mer*, 18, 117–140, 1952.

793 Stukel, M. R.: Investigating equations for measuring dissolved inorganic nutrient uptake in
794 oligotrophic conditions, *Limnol. Oceanogr. Methods*, 18, 656–672, 2020.

795 Suggett, D. J., Stambler, N., Prášil, O., Kolber, Z., Quigg, A., Vázquez-Dominguez, E.,
796 Zohary, T., Berman, T., Iluz, D., Levitan, O., Lawson, T., Meeder, E., Lazar, B., Bar-Zeev,
797 E., Medova, H., and Berman-Frank, I.: Nitrogen and phosphorus limitation of oceanic
798 microbial growth during spring in the Gulf of Aqaba, *Aquat. Microb. Ecol.*, 56, 227–239,
799 2009.

800 Tang, W., Ward, B. B., Beman, M., Bristow, L., Clark, D., Fawcett, S., Frey, C., Fripiat, F.,
801 Herndl, G. J., Mduyana, M., Paulot, F., Peng, X., Santoro, A. E., Shiozaki, T., Sintes, E.,
802 Stock, C., Sun, X., Wan, X. S., Xu, M. N., and Zhang, Y.: Database of nitrification and
803 nitrifiers in the global ocean, *Earth Sci. Rev.*, 15, 5039–5077,
804 <https://doi.org/https://doi.org/10.5194/essd-15-5039-2023>, 2023.

805 Torfstein, A., Teutsch, N., Tirosh, O., Shaked, Y., Rivlin, T., Zipori, A., Stein, M., Lazar, B.,
806 and Erel, Y.: Chemical characterization of atmospheric dust from a weekly time series in the
807 north Red Sea between 2006 and 2010, *Geochim. Cosmochim. Acta*, 211, 373–393,
808 <https://doi.org/10.1016/j.gca.2017.06.007>, 2017.

809 Travis, N. M., Kelly, C. L., and Casciotti, K. L.: Testing the influence of light on nitrite
810 cycling in the eastern tropical North Pacific, *Biogeosciences*, 21, 1985–2004,
811 <https://doi.org/10.5194/bg-21-1985-2024>, 2024.

812 Wan, X. S., Sheng, H.-X., Dai, M., Church, M. J., Zou, W., Li, X., Hutchins, D. A., Ward, B.
813 B., and Kao, S.-J.: Phytoplankton-nitrifier interactions control the geographic distribution of
814 nitrite in the upper ocean, *Global Biogeochem. Cycles*, 35, e2021GB007072,
815 <https://doi.org/https://doi.org/10.1029/2021GB007072>, 2021.

816 Wan, X. S., Sheng, H.-X., Shen, H., Zou, W., Tang, J.-M., Qin, W., Dai, M., Kao, S.-J., and
817 Ward, B. B.: Significance of Urea in Sustaining Nitrite Production by Ammonia Oxidizers in
818 the Oligotrophic Ocean, *Global Biogeochem. Cycles*, 38, e2023GB007996,
819 <https://doi.org/https://doi.org/10.1029/2023GB007996>, 2024.

820 Wankel, S. D., Kendall, C., Pennington, J. T., Chavez, F. P., and Paytan, A.: Nitrification in
821 the euphotic zone as evidenced by nitrate dual isotopic composition: Observations from
822 Monterey Bay , California, *Glob. Biochem. cycles*, 21, 1–13,
823 <https://doi.org/10.1029/2006GB002723>, 2007.

824 Ward, B. B.: Light and substrate concentration relationships with marine ammonium
825 assimilation and oxidation rates, *Mar. Chem.*, 16, 301–316,
826 [https://doi.org/https://doi.org/10.1016/0304-4203\(85\)90052-0](https://doi.org/https://doi.org/10.1016/0304-4203(85)90052-0), 1985.

827 Ward, B. B.: Nitrogen transformations in the Southern California Bight, *Deep Sea Res. Part*
828 *A. Oceanogr. Res. Pap.*, 34, 785–805, [https://doi.org/https://doi.org/10.1016/0198-](https://doi.org/https://doi.org/10.1016/0198-0149(87)90037-9)
829 [0149\(87\)90037-9](https://doi.org/https://doi.org/10.1016/0198-0149(87)90037-9), 1987.

830 Ward, B. B.: Nitrification in Marine Systems, in: *Nitrogen in the Marine Environment*
831 *Environment*, edited by: Capon, D. G., Bronk, D. A., Mulholland, M. R., and Carpenter, E.
832 J., Elsevier, 199–262, <https://doi.org/10.1016/B978-0-12-372522-6.00005-0>, 2008.

833 Welschmeyer, N. A.: Fluorometric analysis of chlorophyll a in the presence of chlorophyll b
834 and pheopigments, *Limnol. Oceanogr.*, 39, 1985–1992, 1994.

835 Wuchter, C., Abbas, B., Coolen, M. J. L., Herfort, L., van Bleijswijk, J., Timmers, P., Strous,
836 M., Teira, E., Herndl, G. J., Middelburg, J. J., Schouten, S., and Sinninghe Damsté, J. S.:
837 Archaeal nitrification in the ocean, *Proc. Natl. Acad. Sci.*, 103, 12317–12322,
838 <https://doi.org/10.1073/pnas.0600756103>, 2006.

839 Xu, M. N., Li, X., Shi, D., Zhang, Y., Dai, M., Huang, T., Glibert, P. M., and Kao, S.-J.:
840 Coupled effect of substrate and light on assimilation and oxidation of regenerated nitrogen in
841 the euphotic ocean, *Limnol. Oceanogr.*, 64, 1270–1283,
842 <https://doi.org/https://doi.org/10.1002/lno.11114>, 2019.

843 Yin, Q., He, K., Collins, G., De Vrieze, J., and Wu, G.: Microbial strategies driving low
844 concentration substrate degradation for sustainable remediation solutions, *npj Clean Water*, 7,
845 52, <https://doi.org/10.1038/s41545-024-00348-z>, 2024.

846 Yool, A., Martin, A. P., Fernández, C., and Clark, D. R.: The significance of nitrification for
847 oceanic new production, *Nature*, 447, 999–1002, <https://doi.org/10.1038/nature05885>, 2007.

848 Zheng, Z.-Z., Wan, X., Xu, M. N., Hsiao, S. S.-Y., Zhang, Y., Zheng, L.-W., Wu, Y., Zou,
849 W., and Kao, S.-J.: Effects of temperature and particles on nitrification in a eutrophic coastal
850 bay in southern China, *J. Geophys. Res. Biogeosciences*, 122, 2325–2337,
851 <https://doi.org/https://doi.org/10.1002/2017JG003871>, 2017.

852 Zheng, Z.-Z., Zheng, L.-W., Xu, M. N., Tan, E., Hutchins, D. A., Deng, W., Zhang, Y., Shi,
853 D., Dai, M., and Kao, S.-J.: Substrate regulation leads to differential responses of microbial
854 ammonia-oxidizing communities to ocean warming, *Nat. Commun.*, 11, 3511,

855 <https://doi.org/10.1038/s41467-020-17366-3>, 2020.

856 Zhou, Y., Yan, A., Yang, J., He, W., Guo, S., Li, Y., Wu, J., Dai, Y., Pan, X., Cui, D.,
857 Pereira, O., Teng, W., Bi, R., Chen, S., Fan, L., Wang, P., Liao, Y., Qin, W., Sui, S.-F., Zhu,
858 Y., Zhang, C., and Liu, Z.: Ultrastructural insights into cellular organization, energy storage
859 and ribosomal dynamics of an ammonia-oxidizing archaeon from oligotrophic oceans, *Front.*
860 *Microbiol.*, 15, 1367658, <https://doi.org/10.3389/fmicb.2024.1367658>, 2024.

861 Zhu, W., Wang, C., Hill, J., He, Y., Tao, B., Mao, Z., and Wu, W.: A missing link in the
862 estuarine nitrogen cycle? Coupled nitrification-denitrification mediated by suspended
863 particulate matter, *Sci. Rep.*, 8, 2282, <https://doi.org/10.1038/s41598-018-20688-4>, 2018.

864